January 2012

Determination of airborne nanoparticles from welding operations

Journal of Toxicology and Environmental Health, Part A: Current Issues
Publication details, including instructions for authors and subscription information:
http://www.tandfonline.com/loi/uteh20

Determination of Airborne Nanoparticles from Welding Operations

João Fernando Pereira Gomes [a b], Paula Cristina Silva Albuquerque [c], Rosa Maria Mendes Miranda [d] & Maria Teresa Freire Vieira [e]

[a] IBB-Instituto de Biotecnologia e Bioengenharia/Instituto Superior Técnico-Universidade Técnica de Lisboa, Lisboa, Portugal

[b] ISEL-Instituto Superior de Engenharia de Lisboa, Área Departamental de Engenharia Química, Lisboa, Portugal

[c] ESTESL-Escola Superior de Tecnologia de Saúde de Lisboa-Instituto Politécnico de Lisboa, Lisboa, Portugal

[d] UNIDEMI, Departamento de Engenharia Mecânica e Industrial, Faculdade de Ciências e Tecnologia, FCT, Universidade Nova de Lisboa, Caparica, Portugal

[e] CEMUC, Departamento de Engenharia Mecânica, Faculdade de Ciências e Tecnologia da Universidade de Coimbra, Coimbra, Portugal

Version of record first published: 12 Jul 2012

To cite this article: João Fernando Pereira Gomes, Paula Cristina Silva Albuquerque, Rosa Maria Mendes Miranda & Maria Teresa Freire Vieira (2012): Determination of Airborne Nanoparticles from Welding Operations, Journal of Toxicology and Environmental Health, Part A: Current Issues, 75:13-15, 747-755

To link to this article: http://dx.doi.org/10.1080/15287394.2012.688489

Journal of Toxicology and Environmental Health, Part A, 75:747–755, 2012

ISSN: 1528-7394 print / 1087-2620 online
DOI: 10.1080/15287394.2012.688489

Taylor & Francis
Taylor & Francis Group

DETERMINATION OF AIRBORNE NANOPARTICLES FROM WELDING OPERATIONS

João Fernando Pereira Gomes[1,2], Paula Cristina Silva Albuquerque[3], Rosa Maria Mendes Miranda[4], Maria Teresa Freire Vieira[5]

[1]IBB–Instituto de Biotecnologia e Bioengenharia/Instituto Superior Técnico–Universidade Técnica de Lisboa, Lisboa, Portugal
[2]ISEL–Instituto Superior de Engenharia de Lisboa, Área Departamental de Engenharia Química, Lisboa, Portugal
[3]ESTESL–Escola Superior de Tecnologia de Saúde de Lisboa–Instituto Politécnico de Lisboa, Lisboa, Portugal
[4]UNIDEMI, Departamento de Engenharia Mecânica e Industrial, Faculdade de Ciências e Tecnologia, FCT, Universidade Nova de Lisboa, Caparica, Portugal
[5]CEMUC, Departamento de Engenharia Mecânica, Faculdade de Ciências e Tecnologia da Universidade de Coimbra, Coimbra, Portugal

The aim of this study is to assess the levels of airborne ultrafine particles emitted in welding processes (tungsten inert gas [TIG], metal active gas [MAG] of carbon steel, and friction stir welding [FSW] of aluminum) in terms of deposited area in pulmonary alveolar tract using a nanoparticle surface area monitor (NSAM) analyzer. The obtained results showed the dependence of process parameters on emitted ultrafine particles and demonstrated the presence of ultrafine particles compared to background levels. Data indicated that the process that resulted in the lowest levels of alveolar deposited surface area (ADSA) was FSW, followed by TIG and MAG. However, all tested processes resulted in significant concentrations of ultrafine particles being deposited in humans lungs of exposed workers.

Welding is the principal industrial process used for joining metals. However, welding may produce dangerous fumes that may be hazardous to the welder's health (Antonini et al 2004; Gomes 1993; Gordon 2004), and it is estimated that presently 1–2% of workers from different professional backgrounds, which accounts for more than 3 million individuals are subjected to welding fume and gas action (Pires et al. 2006). With the advent of new types of welding procedures and consumables, the number of welders exposed to welding fumes is growing constantly despite mechanization and automation of processes (Ascenço et al. 2005). Simultaneously, the number of publications on epidemiologic studies (Pires et al. 2006) and devices for welders' protection is also increasing.

The influence on human health of ultrafine particulate in the nanoparticles range has raised concerns (Jenkins and Eager 2005; Tabet et al 2009) as airborne nanoparticles resulting both from nanotechnologies processes and also from macroscopic common industrial processes such as welding is increasing. In fact, nanotoxicological research is still in its infancy and the issuing and implementation of standards for appropriate safety control systems may still take several years. Yet the advanced understanding of toxicological phenomena at the nanometer scale is largely dependent on technological innovations and scientific results stemming from enhanced research and development (Friedrichs and Schulte 2007). In the interim, industry needs to adopt proactive risk management strategies in order to provide a safe working environment

The authors ACT–Autoridade para as Condições do Trabalho, which partially supported this work under project 035APJ/09.
Address correspondence to João Fernando Pereira Gomes, Chemical Engineering Department, IST–Instituto Superior Técnico, Av. Rovisco Pais, Lisboa 1949-014, Portugal. E-mail: jgomes@deq.isel.ipl.pt

for staff, clients, and customers, and to obtain products without posing adverse health threats at any point of their life cycle. Nanoparticle materials enter the body via three main routes: (a) inhalation, (b) gastrointestinal (GIT), and (c) dermal. The adverse health effects of inhaling fine aerosols were recognized (Maynard and Kuempel 2005) and various attempts have been made to minimize exposure, as the issuing of specific regulations on emissions and objectives for air quality. While toxicological testing of nanoparticles entering dermally or GIT (Friedrichs and Schulte 2007) is still in its infancy, inhalation technology has been concerned with both naturally occurring and engineered nanometer-sized materials. However, most studies resulted in contradictory and controversial conclusions, and little or no standardization of experimental parameters (Adams et al. 1980; Hansen 1989; Henning et al. 2009). In particular, standard toxicology tests were found to be unsuitable to explain toxicity of nanometer-sized particles, leading nanotoxicology laboratories to recommend adoption of another type of metric that takes into account the materials active surface area and structure. Therefore, recent nanotoxicology studies are trying to reach reproducible results by determining the surface effects and other physical parameters of materials. This question is important especially for the European chemical industry due to the Registration, Evaluation, Authorization and Restriction of Chemical Substances (REACH, Regulation EC 1907/2006) regulations. It was recommended that nanoparticulate materials be treated as new substances under the REACH regulation, which supersedes the existing notification of new substances. Studies showed the predominant role of indoor air in personal exposure to many air pollutants (Bruce et al. 2000; Ezzati and Kammen 2002; Spengler and Sexton 1983). These findings may be explained by the high proportion of time that individuals spend indoors and by high concentrations of many air pollutants found there (Bruce et al. 2000). The main issue, in designing exposure assessment studies, is which of the microenvironments where subjects spend their time needs to be studied to provide data allowing for most accurate assessments, while limiting the costs and efforts relating to the studies. When considering human exposures to airborne pollutants the exposure to airborne particles, and especially to its finer fractions—nanoparticles, ultrafine particles, submicrometer particles, $PM_{2.5}$ and PM_{10} fractions—is of particular importance (Kandliker et al. 2007). Obviously, the smaller the particles, the higher is the probability of penetration into deeper parts of the respiratory tract. It should be noted that, in air, smaller and larger particles behave differently, and the penetration of particles of different sizes through the building envelope is also different (Hoet et al. 2004).

Indoor particle concentration is a function of a number of factors, such as the generation rate of particles indoor, outdoor particle concentration, air exchange rate, particle penetration efficiency from outdoor to indoor environment, and particle deposition rate on indoor surfaces. However, in practice, it is usually difficult to assess the exposure due to lack of data and information on the correlation between indoor and outdoor particles, which are house and environment specific. Understanding the relationship of indoor and outdoor aerosol particles, especially in the nano range, under different environmental conditions is of major concern for improving exposure estimates and developing efficient control strategies to reduce human exposure and thus adverse health risk. Current exposure assessment models are often based on outdoor pollutant concentrations used as an input parameter for predicting total exposure. However, indoor concentrations may be different than outdoor ones even in the absence of any significant indoor pollution sources, and this is particularly true when the nano range of particulates is considered.

Occupational health risks associated with manufacturing and use of nanoparticles are not yet clearly understood. However, workers may be exposed to nanoparticles through inhalation at levels that greatly exceed ambient concentrations (Oberdörster 1996). Current workplace exposure limits that have been established are

based on particle mass. However, this criterion does not seem adequate with respect to nanoparticles, as these materials are, in fact, characterized by large surface areas, which are a distinctive characteristic that may even convert an inert substance into another substance, having the same chemical composition but exhibiting different interactions with biological fluids and cells (Oberdörster et al. 1995), which may or not be beneficial. Therefore, it seems that assessing human exposure based on the mass concentration of particles, which is widely adopted for particles over 1 μm, might not be adequate in this particular case. In fact, nanoparticles have greater surface area for the equivalent mass than larger particles, which increases the chance they may react with body tissues (Kreyling et al. 2002). Thus, a growing number of experts (Donaldson et al. 1998; Oberdörster 1996) indicated that surface area needs to be used for nanoparticle exposure and dosing. As a result, assessing workplace conditions and personal exposure based on the measurement of particle surface area is of growing interest.

It is well known that lung deposition is the most efficient way for airborne particles to enter the body and potentially produce adverse health effects (Oberdörster 2001). Properties that contribute to adverse effects of nanoparticles include solubility, particle morphology, particle size, composition, surface chemistry, surface coatings, and surface area (Oberdörster et al. 2005). If nanoparticles can be deposited in lung and remain there, have an active surface chemistry, and interact with the body, then there is potential for exposure and dosing. Oberdörster (2001) showed that surface area plays an important role in the toxicity of nanoparticles and is the measurement metric that best correlates with particle-induced adverse health effects. The potential for adverse health effects is directly proportional to particle surface area (Driscoll 1996).

Mass measurement methods are not sufficiently sensitive for airborne nanoparticles and are not sensitive toward the specific health-relevant properties of nanoparticles (Fissan et al. 2007). The most sensitive concentration measured in this particle range is <100 nm diameter. However, the numerical concentration is dominated by small particles, which are difficult to measure due to increased line losses and reduced counting efficiency with decreased particle size for all counters. Further, it is doubtful if the numerical concentration correlates well with health effects. This seems to be true for asbestos fibers, with a certain probability for each fiber to produce an adverse health effect, and may also be true for nanoparticles in case of agglomeration after penetrating into the blood. Oberdörster (1996) showed that surface area is a relevant metric for nanoparticles, as most of the processes in humans occur via the particle surface, which is increasing significantly with decreasing particle size in the nanometer size range for the same amount of mass. Thus, the adverse health effects after intake are also dependent on the deposition regions. Of particular interest is the deposition in the nose (head), because of possible transfer of nanoparticles to the brain and the tracheobronchial region as well as the alveolar region, because of the inefficiency of clearing mechanisms and the possible transfer to blood circulation system with resulting distribution in several end organs (Kreyling et al. 2002).

In 1996, the International Commission of Radiological Protection (ICRP) developed a comprehensive lung deposition model for radioactive aerosols. Several parameters are required to construct the model, including breathing rate, lung volume, activity, and nose/mouth breathing. The obtained deposition curves (for tracheobronchial and alveolar deposition) derived from the model vary according to these parameters. For industrial hygiene applications, American Conference of Government Industrial Hygienists (ACGIH) (Phalen 1999) developed a definition of a reference worker, as follows, in order to derive the deposition curves:

a. Physiological parameters
   Subject: adult male
   Functional residual capacity: 2200 cm^3
   Extra-thoracic dead space: 50 cm^3
   Bronchial dead space: 49 cm^3

Bronchiolar dead space: 47 cm^3
Height: 175 cm
Tracheal diameter: 1.65 cm
First bronchial diameter: 0.165 cm

b. Activity-related parameters
Activity level: light exercise
Activity type: nose breathing only
Ventilation rate: 1.3 m^3/h
Respiratory frequency: 15.0 breaths/min
Tidal volume: 1450 cm^3
Volumetric flow rate: 725 cm^3/s
Fraction breathed through nose: 1

c. Aerosol parameters
Activity mean aerodynamic diameter: 0.001 μm–0.5 μm
Geometric standard deviation: 1
Density: 1 g/cm^3
Shape factor: 1

The tracheobronchial deposition curve represents the fraction of aerosol that deposits in the tracheobronchial region of the lung, and the alveolar deposition curve represents the fraction of the aerosol that deposits in the alveolar region of the lung. For exposure assessment applications it is common to sample aerosols relevant to their deposition in a specific region of the human lung, which is often referred to as size-selective health hazard sampling. The criterion for size-selective sampling depends on the aerosol being sampled. Withy respect to nanoparticles, the adverse health effects relate to the deposition deep in the alveolar regions of the lung, and thus the respirable fraction of the aerosol is the metric of interest.

MATERIALS AND METHODS

For measuring nanoparticle exposure, a nanoparticle surface area monitor, TSI, model 3550, was used. This equipment indicates the human lung-deposited surface area of particles expressed as square micrometers per cubic centimeter of air ($\mu m^2/cm^3$), corresponding to tracheobronchial (TB) and alveolar (A) regions of the lung. This equipment is based on diffusion charging of sampled particles, followed by detection of the charged aerosol using an electrometer. Using an integral pump, an aerosol sample is drawn into the instrument through a cyclone with a 1-μm cut point. The sample flow is split, with one stream going through a set of carbon and HEPA filters and an ionizer to introduce positively charged ions into a mixing chamber. The other aerosol flow stream is mixed with the ionized stream in a mixing chamber, and charged aerosol and excess ions move onto an ion trap. The ion trap voltage can be set to TB or A response. The ion trap acts as an inlet conditioner or a size-selective sampler for the electrometer, by collecting the excess ions and particles that are not of a charged state, corresponding to the TB or A response settings. The aerosol then moves on to the electrometer for charge measurement, where current is passed from the particles to a conductive filter and measured by a sensitive amplifier, as depicted schematically in Figure 1. The charge measured by the electrometer is directly proportional to the surface area of the particles passing through the electrometer. The equipment, when set to A response settings, matches the corresponding lung deposition criteria of particles for a reference worker predicted by human lung deposition models from ICRP and ACGIH.

Tests for exposure assessment were made over three different welding processes: metal active gas (MAG) and tungsten inert gas (TIG) on carbon steel (in both cases), and friction stir welding (FSW) of aluminum alloy AA7178, using different welding parameters and also different sampling locations. The measured deposited area was expressed as alveolar due to the reduced size of the emitted particles. Due to the inexistence of an exposure limit value, for each measurement task a baseline value was obtained for comparison purposes. MAG welding was performed with a PROMIG Kempi machine using an AWS 70S filler with 0.8 mm diameter of 6 m/min feeding rate under a gas protection of CO_2 + 15% Ar at 10 L/min flow rate. Three current intensities were tested, 120, 210, and 285 A, in order to produce short-circuit, globular, and spray-metal transfer modes. Beads on the plate were produced in all cases. TIG welding was performed on carbon steel with three current intensities, 90,

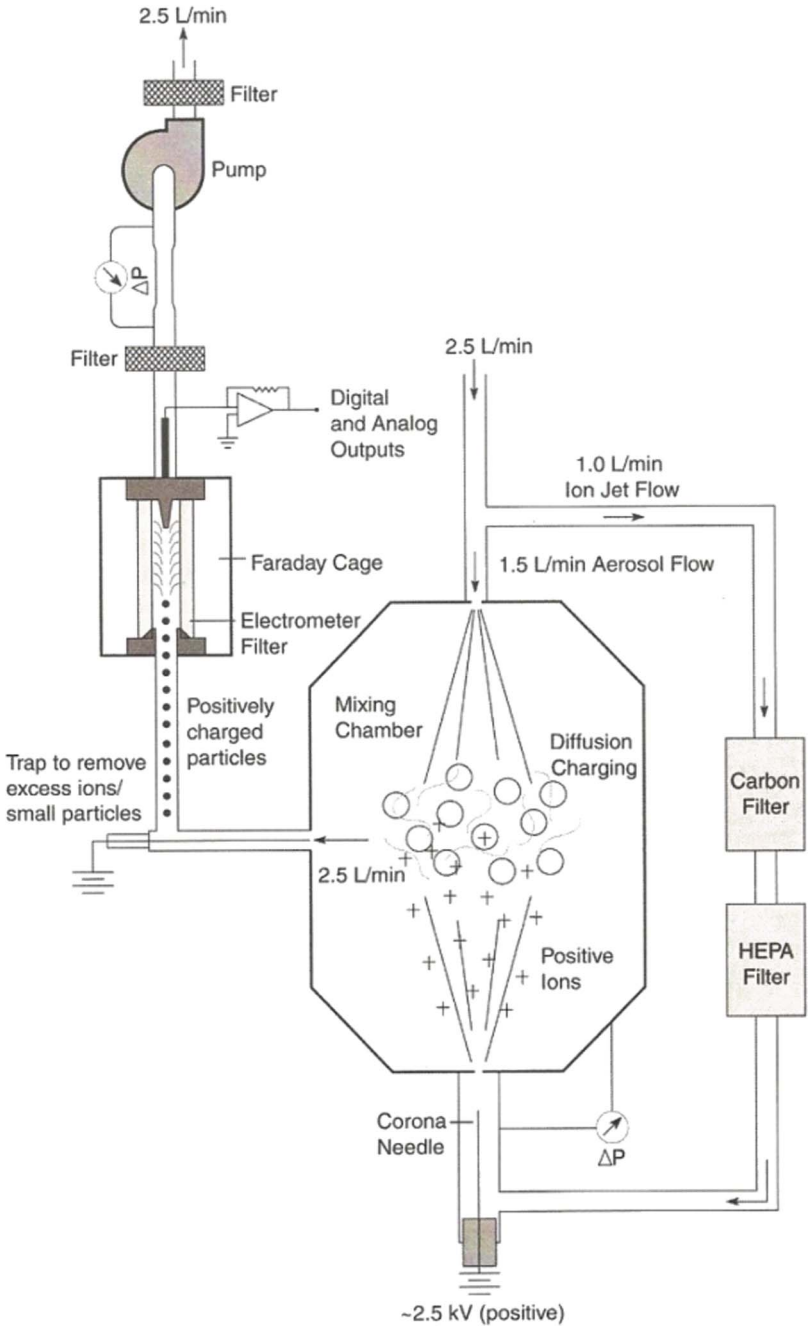

FIGURE 1. Schematic of the Nanoparticle Surface Area Monitor operation (color figure available online).

120, and 210 A, with a nonconsumable thorium electrode under argon protection flowing at 10 L/min through a nozzle of 5 mm diameter. FSW was performed in AA7178-T6 with a conical threaded probe and a shoulder having a spiral scrolled profile, with a traverse speed (V) of 355 and 180 mm/min and a rotation speed (Ω) of 355 and 1120 rev/mm, that is, with V/Ω ratios of 1 and 6, respectively, in the cold and hot condition. Sampling was taken at different locations inside the welder mask for MAG and TIG welding, and at 30 and 60 cm from the weld zone. In FSW, sampling was done close to the shoulder.

RESULTS AND DISCUSSION

Table 1 shows the measured values for MAG welding of carbon steel. In terms of process parameters, the largest values were obtained for the highest current intensity tested of 285 A, when compared to the lowest intensities of 210 and 120 A. This was to be expected, as noted by Jenkins and Eager (2005) that the more energy-intensive welding processes are, the higher are the amounts of airborne particles emitted.

Pires et al. (2007) studied the metal transfer mode in MAG welding and the effect of both gas mixture and processing parameters on the fume formation rate. The metal transfer mode is influenced by the type of the filler wire, voltages and current intensities range, electrode polarity, and shielding gas. The arc stability decreases with the rise in carbon dioxide (CO_2) content in the mixture. This fact is related to the high thermal conductivity of CO_2, which gives rise to more heat loses by conduction and thus the necessity to use higher voltages, for the same current intensity, to initiate and stabilize the arc. Due to the greater heat flow associated with gas mixtures with higher content of CO_2, the radial distribution of the arc temperature is more uniform and its length is shorter for the same current intensity. In contrast, mixtures with less CO_2 have an inner zone that is much hotter than the peripheral zone. It was also observed that the extension of the spray transfer region decreases with elevated CO_2 content. This phenomenon is also related to the rise of thermal conductivity of the mixture, with increasing CO_2 content. As the thermal conductivity of the mixture rises, the arc stops enveloping the droplet, producing an anodic spot contraction, and results in a shorter electric conduction zone. The reduction of the conduction zone with the increase of CO_2 content also produces an expansion of the area where repelled transfer mode occurs. The vaporization force, mainly responsible for this type of transfer mode, is the result not only of the reduction of the conduction zone, but also of the extremely active behavior of CO_2. The CO_2 reacts either with the weld pool elements or with the electrode elements, leading to the formation of extremely volatile oxides. This study provided information on the evolution of fume formation rate with the current intensity, for the gas mixtures studied. The fume formation rate increases with the increase of CO_2 in the mixture. The fume formation rate increases with the rise in arc temperature and instability, with the active component, with thermal conductivity of the mixture, and with the volume of the droplets. The amount of fume released during welding is higher for mixtures with CO_2 relative to the ones with O_2 having the same oxidizing potential. Differences in the measured values were also observed in relation to the sampling

TABLE 1. Measurements for MAG Welding of Carbon Steel

Welding conditions	Sampling location	Average deposited area ($\mu m^2/cm^3$)	Minimum and maximum values ($\mu m^2/cm^3$)	TWA for 8 h ($\mu m^2/cm^3$)	Total deposited area (μm^2)	Dose per lung area ($\mu m^2/m^2$)
No welding, baseline	—	107.8	67.2–193.9	2.99	1.44×10^6	1.80×10^4
120 A	Welder mask	24,300	7270–66,400	75.9	3.64×10^7	4.55×10^5
210 A	Welder mask	69,100	42,100–92,200	120.0	$5{,}76 \times 10^7$	7.20×10^5
285 A	Welder mask	96,400	82,600–100,000	234.2	1.12×10^8	1.41×10^6
210 A	30 cm from welding	840.5	452.5–1050	2.63	1.26×10^6	1.58×10^4
120 A	60 cm from welding	353.0	309.4–378.8	0.98	4.71×10^5	5.88×10^3
210 A	60 cm from welding	833.6	765.8–916.7	2.03	9.73×10^5	1.22×10^4
285 A	60 cm from welding	1070	946.7–1180	2.22	1.07×10^6	1.33×10^4

TABLE 2. Measurements for TIG Welding of Carbon Steel

Welding conditions	Sampling location	Average deposited area ($\mu m^2/cm^3$)	Minimum and maximum values ($\mu m^2/cm^3$)	TWA for 8 h ($\mu m^2/cm^3$)	Total deposited area (μm^2)	Dose per lung area ($\mu m^2/m^2$)
No welding, baseline	—	134.8	126.9–144.4	2.15	1.03×10^6	1.29×10^4
120 A	Welder mask	6240	117.9–23300	54.2	2.60×10^7	3.25×10^5
90 A	60 cm from welding	158.6	112.8–329.9	1.65	7.93×10^5	9.91×10^3
120 A	60 cm from welding	174.7	124.9–256.4	0.97	4.66×10^5	5.28×10^3
210 A	60 cm from welding	503.4	353.5–1080	3.15	1.51×10^6	1.89×10^4

TABLE 3. Measurements for FSW of Aluminum

Welding conditions	Sampling location	Average deposited area ($\mu m^2/cm^3$)	Minimum and maximum values ($\mu m^2/cm^3$)	TWA for 8 h ($\mu m^2/cm^3$)	Total deposited area (μm^2)	Dose per lung area ($\mu m^2/m^2$)
No welding, baseline	—	64.0	61.5–68.0	2.11	1.01×10^6	$1,27 \times 10^4$
180 mm/mmCold	Welding tool	10,600	11.0–42,500	40.6	1.95×10^7	2.44×10^5
355 mm/mmCold	Welding tool	2500	56.0–13,900	6.95	3.34×10^6	4.17×10^4
180 mm/mmHot	Welding tool	16,500	59.4–100,000	160.3	7.70×10^7	9.62×10^5
355 mm/mmHot	Welding tool	15,700	38.6–100,000	114.5	5.49×10^7	6.87×10^5

location. As expected, the highest values were obtained near the welding front, and as the sampling port was farther from the welding front, lower values were observed. Values measured inside the welder mask are high, which is due to the existence of a confined location as opposed to outside locations where particle dispersion can easily occur. Nevertheless, it should be noted that the particular masks used by the welder in this situation are mainly designed to protect the welder from ultraviolet (UV) radiation and not from airborne emissions.

Table 2 shows the measured values for TIG welding of carbon steel with intensities varying from 90 to 210 A. Again, higher values are obtained with greater current intensities. Measurements were also performed for friction stir welding of aluminum, which Nicholas (1998) indicated was a cleaner welding process, as this process does not involves the use of electric current nor the actual fusion and deposition of metal associated with the majority of welding processes. Concerning this process, two different tool velocities were tested. Even for this process, elevated values were measured. As expected, the higher values are obtained for greater velocity of the tool and also for hot operation in comparison with cold operation, as shown in Table 3. Performed sampling periods were usually small but, nevertheless, certain variations over the measured values could be observed during sampling, as shown in Figure 2.

CONCLUSIONS

This set of measurements is the first stage of a study on airborne particles emitted in welding processes. The study clearly demonstrated the existence of nanoparticles in MAG and TIG welding of carbon steel, as well as in FSW of aluminum, which are clearly dependent on the distance to the welding front and also on the main welding parameters, namely, the welding current. The emission of airborne particles rose with current intensity as fume formation rate. An exponential decay of nanoparticles with the distance to the weld area was observed.

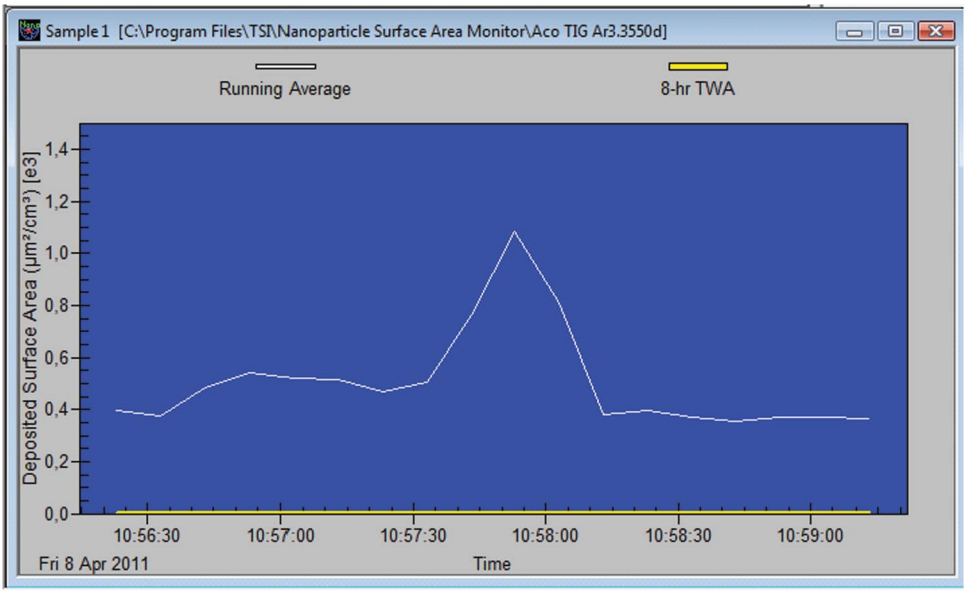

FIGURE 2. Measured values during TIG welding: welding took place from 10:57:05 to 10:58:10 (color figure available online).

It should be noted that although measured parameters such as the deposited area and the dose per lung area are elevated when compared with baseline values, these cannot, at this stage, be ascertained as toxicity indicators. These preliminary measurements have to be complemented with the size distribution of airborne nanoparticles and also the chemical composition and information on the shape and crystalline nature of these particles.

REFERENCES

Adams, H., Feuerstein, M., and Fowler, J. 1980. Migraine headache: Review of parameters, etiology, and intervention. *Psychol. Bull*. 87: 217–37.

Antonini, J. M., Taylor, M. D., Zimmer, A. T., and Roberts, J. R. 2004. Pulmonary responses to welding fumes: Role of metal constituents. *J. Toxicol. Environ. Health A* 67: 233–49.

Ascenço, C., Gomes, J., Cosme, N., and Miranda, R. 2005. Analysis of welding fumes. *Toxicol. Environ. Chem*. 87: 345–49.

Bruce, N., Padilla, R., and Albalak, R. 2000. Indoor air pollution in developing countries: A major environmental and public health challenge. *Bull. WHO* 78: 1078–92.

Donaldson, K., Li, X., and MacNee, W. 1998. Ultrafine (nanometer) particle mediated lung injury. *J. Aerosol Sci*. 29: 553–560.

Driscoll, K. 1996. Role of inflammation in the development of rat lung tumors in response to chronic particle exposure. *Inhal. Toxicol*. 8: 85–98.

Ezzati, M., and Kammen, D. 2002. Household energy, indoor air pollution and health in developing countries: Knowledge base for effective interventions. *Annu. Rev. Energy Environ.* 27: 233–70.

Fissan, H., Neumann, S., Trampe, A., Pui, D., and Shin, W. 2007. Rationale and principle of an instrument measuring lung deposited nanoparticle surface area. *J. Nanoparticle Res*. 9: 53–59.

Friederichs, S., and Schulte, J. 2007. Environmental, health and safety aspects of nanotechnology—Implications for the R&D in (small) companies. *Sci. Technol. Adv. Mater.* 8: 12–18.

Gomes, J. 1993. *Higiene e Segurança da Soldadura*. Oeiras, Portugal: Ed. ISQ.

Gordon, T. 2004. Metalworking fluid—The toxicity of a complex mixture. *J. Toxicol. Environ. Health A* 67: 209–19.

Hansen, C. 1989. A causal model of the relationship among accidents, biodata,

personality, and cognitive factors. *J. Appl. Psychol*. 74: 81–90.
Henning, A., Schaefer, U., and Neumann, D. 2009. Potential pitfalls in skin permeation experiments: Influence of experimental factors and subsequent data evaluation. *Eur. J. Pharm. Biopharm*. 72: 324–31.
Hoet, P., Hohlfeld, I., and Salata, O. 2004. Nanoparticles—Known and unknown health risks. *J. Nanobiotechnol*. 2: 12.
Jenkins, N., and Eager, T. 2005. Chemical analysis of welding fume particles, *Welding J. Suppl*. 87–93.
Kandliker, M., Ramachandran, G., Maynard, A., Murdock, B., and Toscano, W. 2007. Health risk assessment for nanoparticles: A case for using expert judgment. *Nanotechnol. Occup. Health* 3: 137–56.
Kreyling, W., Semmler, M., Erbe, F., Mayer, P., Takenaka, S., Schulz, H., Oberdörster, G., and Ziesenis, A. 2002. Translocation of ultrafine insoluble iridium particles from lung epithelium to extrapulmonary organs is size dependent but very low. *J. Toxicol. Environ. Health A* 65: 511–35.
Maynard, A., and Kuempel, E. 2005. Airborne nanostructured particles and occupational health. *J. Nanoparticle Res*. 7: 587–614.
Nicholas, E. 1998. *Developments in the friction-stir welding of metals*. ICAA-6: 6th International Conference on Aluminium Alloys, Toyohashi, Japan.
Oberdörster, G., Gelein, R., Ferin, J., and Weiss, B. 1995. Association of particulate air pollution and acute mortality: Involvement of ultrafine particles. *Inhal. Toxicol*. 7: 111–124.
Oberdörster, G. 1996. Significance of particle parameters in the evaluation of exposure-dose-response relationships of inhaled particles. *Part. Sci. Technol*. 14: 135–151.
Oberdörster, G. 2001. Pulmonary effects of inhaled ultrafine particles. *Int. Arch. Occup. Environ. Health* 74: 1–8.
Oberdörster, G., Maynard, A., Donaldson, K., Castranova, V., Fitzpatrick, J., Ausman, K., Carter, J., Karn, B., Kreyling, W., Lai, D., Olin, S., Riviere, N., Warheit, D., and Yang, H. 2005. Principles for characterizing the potential human health effects from exposure to nanomaterials: Elements of a screening strategy. *Part. Fibre Toxicol*. 2: 8.
Phalen, R. 1999. *Particle Size-selective sampling for particulate air contaminants*. Cincinnati, OH: ACGIH.
Pires, I., Quintino, L., Miranda, R., and Gomes, J. 2006. Fume emissions during gas metal arc welding. *Toxicol. Environ. Chem*. 88: 385–94.
Pires, I., Quintino, L., and Miranda, R. 2007. Analysis of the influence of shielding gas mixtures on the gas metal arc welding metal transfer modes and fume formation rate. *Mater. Design* 28: 1623–31.
Spengler, J., and Sexton, K. 1983. Indoor air pollution: A public health perspective. *Science* 221: 9–17.
Tabet, L., Bussy, C., Amara, N., Setyan, A., Grodet, A., Rossi, M.J., Pairon, J.-C., Boczkowski, J., and Lanone, S. 2009. Adverse effects of industrial multiwalled carbon nanotubes on human pulmonary cells. *J. Toxicol. Environ. Health A* 72: 60–73.